A cost-effective strategy for nonoscillatory convection without clipping

Article · April 1990

Source: NTRS

2 authors:

Brian Phillip Leonard
University of Akron
74 PUBLICATIONS   **6,979** CITATIONS

SEE PROFILE

Hassan Niknafs
Khazar University
10 PUBLICATIONS   **83** CITATIONS

SEE PROFILE

Some of the authors of this publication are also working on these related projects:

Project   Avogadro number = gram-to-dalton mass ratio. View project

Project   The SI 'radian' and 'steradian' cannot be defined as coherent SI derived units. View project

A Cost-Effective Strategy for Nonoscillatory Convection Without Clipping

B.P. Leonard
Institute for Computational Mechanics in Propulsion
Lewis Research Center
Cleveland, Ohio

and

H.S. Niknafs
The Norton Company
Stow, Ohio

NASA

LEWIS RESEARCH CENTER
ICOMP
CASE WESTERN
RESERVE UNIVERSITY

A COST-EFFECTIVE STRATEGY FOR NONOSCILLATORY CONVECTION WITHOUT CLIPPING

B.P. Leonard*
Institute for Computational Mechanics in Propulsion
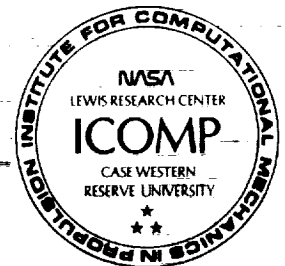Lewis Research Center
Cleveland, Ohio 44135

and

H.S. Niknafs**
The Norton Company
Chemical Products Division
Stow, Ohio 44224

SUMMARY

Clipping of narrow extrema and distortion of smooth profiles is a well-known problem associated with so-called "high-resolution" nonoscillatory convection schemes. In this report, a strategy is presented for accurately simulating highly convective flows containing discontinuities such as density fronts or shock waves, without distorting smooth profiles or clipping narrow local extrema. The convection algorithm is based on non-artificially-diffusive third-order upwinding in smooth regions, with automatic adaptive stencil expansion to (in principle, arbitrarily) higher order upwinding locally, in regions of rapidly changing gradients. This is highly cost-effective because the wider stencil is used only where needed – in isolated narrow regions. A recently developed universal limiter assures sharp monotonic resolution of discontinuities without introducing artificial diffusion or numerical compression. An adaptive discriminator is constructed to distinguish between spurious overshoots and physical peaks; this automatically relaxes the limiter near local turning points, thereby avoiding loss of resolution in narrow extrema. Examples are given for one-dimensional pure convection of scalar profiles at constant velocity.

INTRODUCTION

Accurate simulation of highly convective flows continues to be one of the most challenging problems in computational mechanics. The inability to adequately simulate simple scalar profiles even in the superficially straight-forward case of one-dimensional pure convection at constant velocity has been referred to as the "ultimate embarrassment" for computational mechanics [1]. Classical (second-order central) schemes are able to handle very smooth profiles fairly satisfactorily; i.e., when the convected variable has small curvature (spatial second derivatives) – or, more specifically, when the shortest Fourier components have wavelengths of many mesh-widths. But a sudden change in gradient (involving locally high curvature or short wavelengths) excites spurious unphysical oscillations due to inherent spatial (third-derivative) dispersion terms in the truncation error. By contrast, first-order upwinding [2] can resolve a step profile monotonically, giving a spreading error-function in the idealized case; but the inherent spatial second-derivative (artificial diffusion) terms in the truncation error so totally overwhelm any physical diffusion that even smoothly varying profiles are unrecognizable after a short time.

Second-order upwinding [3] represents a significant improvement. In this case, leading order truncation error is again a dispersive third derivative but, compared with second-order central, fourth- (and higher even-) derivative dissipation terms may be stronger under certain conditions, thus tending to somewhat dampen dispersive oscillations. By averaging second-order upwinding with the canonical explicit second-order central scheme [4], Fromm [3] proposed a convection algorithm in which the leading phase error of the upwind scheme approximately cancels the lagging phase error of the central scheme. However, using the same computational stencil, it is a simple matter to eliminate the third-derivative dispersion term entirely.

The QUICKEST scheme [5] is the canonical explicit third-order upwind convection algorithm of this type; physical diffusion terms are modelled to a consistent order. In this case, the leading truncation-error term is a dissipative (but not diffusive) spatial fourth derivative. This is an important attribute. Numerical experience over the past decade or more has led to the following rule of thumb: leading truncation error in a convection algorithm should be dissipative (an even spatial derivative) rather than dispersive (odd derivative) but should be of higher order than other modelled physical terms such as diffusion (especially if these terms are supposed to be small). Thus, even-order schemes fail the first criterion (central schemes are worse in this respect because dissipative terms are small or non-existent). First-order upwinding fails the second criterion. Third-order upwinding is therefore the lowest order method satisfying both criteria for the convection-diffusion equation. This is especially important for convection-dominated flows, as will be seen in the model test problems shown later.

Unfortunately, third-order upwinding does not seem to have been widely adopted by the computational-fluid-dynamics (CFD) community. Apparently for no other reasons than tradition and personal inertia, many CFD researchers regard second-order central schemes as the norm. This is appropriate for physical problems dominated by *even* spatial derivatives, such as diffusion, wave-motion, and elasticity, but is singularly inappropriate for the *first*-derivative convection term in fluid mechanics [6]. A similar situation occurs with higher order odd derivatives such as the spatial third derivative in the Korteweg-deVries equation [7]. Another large segment of the CFD community (especially in heat-transfer applications) has adopted first-order upwinding as the "safest" form of convection modelling. This

2

apparently stems from the influence of the Imperial College school through descendants of the TEACH code [8] using the "Hybrid" convection scheme [9] or variants of the so-called "exponential difference scheme" [10], including the "power-law" approximation described in a well-known textbook [11]. The difficulty with such an approach is very simple: using these methods, one is not simulating the correct physical problem! A very-high-Reynolds-number (convection-dominated) problem is arbitrarily replaced by an unphysical problem in which the effective component grid Reynolds number can never be greater than 2, whereas the physical grid Reynolds number might be hundreds or thousands (or effectively infinite).

There is also a serious logical flaw in such methods: sophisticated (and expensive) multi-equation turbulence models are usually used at each time or iteration step simply as a diagnostic to *switch off their own effects* in the turbulent-transport terms of the governing equations, replacing these terms with artificial viscosity or diffusivity [12]. Specifically, the turbulence model is used to calculate the (turbulent) component grid Reynolds (or Peclet) number at each control-volume face; when this quantity exceeds 2 (in the case of Hybrid) or about 6 (for the exponential or power-law schemes), physical turbulent transport is replaced by artificial numerical viscosity (or diffusivity). The short-comings of first-order methods are well known, having been shown theoretically [13-15] and through comparative benchmark problems [16-17]. Their continued wide-spread popularity is perhaps another manifestation of the ultimate embarrassment.

Although third-order upwinding is a more rational basis for CFD, certain fundamental problems remain. Perhaps the most obvious is the fact that unphysical overshoots and undershoots are excited each side of a step discontinuity in purely convective flow [5]. And, of course, short-wavelength resolution is limited by the third-order accuracy. Switching to higher order (upwind) schemes can increase accuracy of resolution but cannot reduce the overshoot problem (in fact, it gets slightly worse). Monotonic high resolution schemes can be constructed for simulating step discontinuities. This is usually achieved by using a subtle nonlinear blending of a (traditional) second-order central base scheme with first-order upwinding (introducing enough positive artificial diffusion locally to maintain monotonicity) and first-order downwinding (with inherent *negative* artificial diffusion to locally enhance artificial "compression"). This strategy is the basis of so-called "shock-capturing" and "total-variation-diminishing (TVD)" schemes [18], and can be related to earlier multi-step flux-correction first/second-order schemes [19] and single-step nonlinear flux-limiting schemes such as the second-order MUSCL scheme [20] – a monotonized version of Fromm's method – and the third-order EULER scheme based on exponential upwinding [21,22]. Unfortunately, the best step-resolution (supercompressive) schemes such as Superbee [23], Super-C, or Hyper-C [24], tend to convert smooth profiles into a series of steps and plateaus. In other words, the negative diffusivity responsible for artificial compression of discontinuities tends to concentrate moderate-curvature regions into localized unphysical sharp changes in gradient. All such first/second-order schemes strongly "clip" narrow extrema.

Recently, a universal limiter (UL) has been designed which can be applied to arbitrarily high order transient interpolation modelling (TIM) of the advective transport equations (ATE). This "ULTIMATE" CFD scheme [24] has several attractive properties. Step resolution is monotonic and can be made competitive with the best supercompressive shock-capturing schemes without introducing artificial diffusivity or viscosity, simply by locally increasing the order of accuracy, using adaptive stencil expansion (so that the location of the wider stencil automatically moves

along with high-curvature regions of the profile). Since numerical compression is avoided, smooth profiles are not corrupted. However, one annoying problem remains: very narrow extrema are slightly clipped relative to what can be achieved with an unlimited higher order (upwind) scheme. Near sudden changes in gradient, the limiter needs to be "on", but near local physical extrema (but not spurious overshoots), it needs to be switched "off" automatically. The problem is one of pattern recognition. This paper describes a simple adaptive discriminator which can identify well-defined local narrow physical extrema and automatically switch off the universal limiter in such regions, but keep it activated in regions where unphysical overshoots or very short-wavelength spurious oscillations would otherwise occur.

The overall strategy is as follows:

(i)   In "smooth" regions (identified by small values of local absolute curvature of the convected variable), the unlimited third-order upwind QUICKEST scheme is used; this accounts for the overwhelming bulk of the flow domain – especially in multidimensional flows.

(ii)   In relatively large-gradient or strong-curvature regions, automatic adaptive stencil expansion occurs locally, using (in principle, arbitrarily) higher order upwinding with the universal limiter activated.

(iii) Near well-defined local extrema, identified by the automatic discriminator, the limiter is switched off, thus allowing an appropriate degree of resolution depending on the narrowness of the extremum.

The next section summarizes the basic ideas underlying the universal limiter. Then four challenging scalar test profiles are considered under conditions of pure one-dimensional convection at constant velocity. Results for a number of solution methods are shown in order to demonstrate some of the difficulties mentioned above with respect to various manifestations of the ultimate embarrassment. Construction of the automatic discriminator is then briefly described. Finally, results are shown for a cost-effective variable-order scheme consisting of QUICKEST in smooth regions, ULTIMATE seventh-order upwinding in moderate-curvature regions and ULTIMATE ninth-order upwinding in high-curvature or high-gradient regions.

UNIVERSAL LIMITER

Details of the ULTIMATE scheme can be found elsewhere [24]; however, a brief description of the universal limiter is given here for convenience. Figure 1 shows a one-dimensional control volume, suggesting the local behaviour of the convected variable ϕ in terms of locally normalized variables [22]

$$\widetilde{\phi} = (\phi - \phi_U)/(\phi_D - \phi_U) \tag{1}$$

where ϕ_U is the (unnormalized) upstream node value and ϕ_D the downstream value. Note from Equation (1) and the figure that, in terms of normalized variables,

$$\widetilde{\phi}_U = 0 \quad \text{and} \quad \widetilde{\phi}_D = 1 \tag{2}$$

Let $\widetilde{\phi}_f$ be the normalized face value on the downstream control-volume face; similarly, $\widetilde{\phi}_u$ is the normalized upstream face value. Figure 1 shows interpolative constraints on $\widetilde{\phi}_f$ and $\widetilde{\phi}_u$; i.e.,

4

$$\widetilde{\phi}_C{}^n \leq \widetilde{\phi}_f \leq 1 \qquad (3)$$

and

$$0 \leq \widetilde{\phi}_u \leq \widetilde{\phi}_C{}^n \qquad (4)$$

where $\widetilde{\phi}_C{}^n$ is the normalized central node value. The inequalities given by (3) are two necessary conditions on $\widetilde{\phi}_f$ prescribed by the universal limiter when local behaviour is monotonic across the three nodes shown in Figure 1, i.e., the two nodes straddling the face in question and the adjacent upstream node. However, this is not enough to guarantee computational monotonicity. For this, consider the explicit update step for $\widetilde{\phi}_C$ under conditions of constant velocity (positive to the right in Figure 1). In terms of normalized variables,

$$\widetilde{\phi}_C{}^{n+1} = \widetilde{\phi}_C{}^n - c\,(\widetilde{\phi}_f - \widetilde{\phi}_u) \qquad (5)$$

where $c = u\Delta t/\Delta x$ is the Courant number.

In order to maintain monotonicity (locally), $\widetilde{\phi}_C$ must satisfy

$$\widetilde{\phi}_U{}^{n+1} \leq \widetilde{\phi}_C{}^{n+1} \leq \widetilde{\phi}_D{}^{n+1} \qquad (6)$$

Taking conservative worst-case conditions implies

$$0 \leq \widetilde{\phi}_C{}^{n+1} \leq 1 \qquad (7)$$

The right-hand inequality is assured by the interpolative constraints on $\widetilde{\phi}_f$ and $\widetilde{\phi}_u$; the left-hand inequality implies, using Equation (5),

$$\widetilde{\phi}_f \leq \widetilde{\phi}_u + \widetilde{\phi}_C{}^n/c \qquad (8)$$

Once again, a worst-case estimate for $\widetilde{\phi}_u$ ($=0$) results in an additional (time-step) constraint on $\widetilde{\phi}_f$:

$$\widetilde{\phi}_f \leq \widetilde{\phi}_C{}^n/c \qquad (9)$$

Inequalities (3) and (9) constitute the universal limiter constraints on $\widetilde{\phi}_f$ with respect to $\widetilde{\phi}_C{}^n$ when $\widetilde{\phi}_C{}^n$ is within the monotonic range:

$$0 \leq \widetilde{\phi}_C{}^n \leq 1 \qquad (10)$$

Outside of this range (i.e., $\widetilde{\phi}_C{}^n < 0$ or $\widetilde{\phi}_C{}^n > 1$), various strategies can be devised. Figure 2 shows one simple possibility:

$$\widetilde{\phi}_f = \widetilde{\phi}_C{}^n \quad \text{(nonmonotonic range)} \qquad (11)$$

together with the monotonicity constraints. This is a graphical portrayal of the universal limiter. Using this limiter, the procedure is as follows:

(i) Construct an explicit estimate for the unnormalized control-volume face value, ϕ_f, by any (in principle, arbitrarily high order) method.

(ii) Compute the corresponding normalized value, $\widetilde{\phi}_f$, according to Equation (1).

(iii) If the point ($\widetilde{\phi}_C{}^n$, $\widetilde{\phi}_f$) lies within the shaded region of Figure 2, proceed with the unadjusted face value, $\widetilde{\phi}_f$.

(iv) If the point lies outside this region, replace $\widetilde{\phi}_f$ with the nearest allowable $\widetilde{\phi}_f$ value at the same $\widetilde{\phi}_C{}^n$.

(v) Reconstruct $\phi_f = \phi_U + \widetilde{\phi}_f (\phi_D - \phi_U)$.

(vi) Repeat for each control-volume face.

Note that this strategy is significantly different from that used in currently popular shock-capturing and TVD schemes [18]. In such schemes, using the present normalized-variable terminology,

$$\widetilde{\phi}_f = c\,\widetilde{\phi}_C{}^n + (1-c)\,\widetilde{\phi}_f{}^n \tag{12}$$

where $\widetilde{\phi}_f{}^n$ is a single-valued monotonic function of $\widetilde{\phi}_C{}^n$ passing through the points (0,0), (0.5, 0.75), and (1,1). This restricts such methods to second (or, at best) third order accuracy in space, and second order in time. Figure 3 shows the functional form of $\widetilde{\phi}_f{}^n(\widetilde{\phi}_C{}^n)$ for three well-known methods: Roe's Minmod and Superbee [23], and van Leer's MUSCL [20]. As commonly used in shock-capturing schemes, the TVD limiter [25] can be described by

$$\widetilde{\phi}_C{}^n \leq \widetilde{\phi}_f{}^n \leq \min(2\widetilde{\phi}_C{}^n, 1) \tag{13}$$

in the monotonic range, with $\widetilde{\phi}_f{}^n = \widetilde{\phi}_C{}^n$ elsewhere. These constraints, together with Equation (12), represent much more restrictive conditions than those of the universal limiter [24]. An important point to stress is that the universal limiter can be used with arbitrarily high order (in both space and time) explicit methods whereas the usual TVD strategy is restricted to essentially second order.

CONVECTION OF SCALAR PROFILES

Consider one-dimensional constant-velocity pure convection (i.e., no diffusion) of a scalar profile initially given by

$$\phi(x,0) = \phi_0(x) \tag{14}$$

After time t, the exact solution is the initial profile translated by a distance ut, where u is the convecting velocity; i.e.,

$$\phi(x,t) = \phi_0(x-ut) \tag{15}$$

Figure 4 shows the exact solution of four test profiles under uniform convection to the right. Discontinuity resolution is tested by a simple step rather than the square wave used by some authors [25] (at best, a square wave simply gives twice as much information as a step; for the more dispersive schemes, oscillations produced by the square-wave's step-up can interfere with those produced by the step-down, thus producing a confusing interaction pattern). Smooth behaviour is represented by an isolated sine-squared wave $20\Delta x$ wide; there is no discontinuity in value or gradient, but there is a discontinuity in curvature at each side of the profile. A semi-ellipse $20\Delta x$ wide is very challenging because of a combination of sudden and gradual changes in gradient. A narrow Gaussian with $\sigma = 1.94\Delta x$ has been chosen to test narrow peak resolution.

In the following simulations, the Courant number for all cases is

$$c = 0.45 \qquad (16)$$

Calculations are run for 100 time-steps, so that exact solutions should have shifted 45 mesh-widths to the right. The exact solutions are shown for reference in each case. All of the schemes have been programmed in conservative control-volume form, so that "mass" is conserved (to machine accuracy) in all cases. Upstream ($\phi = 1$) and downstream ($\phi = 0$) boundaries are sufficiently far away (beyond the region shown in the figures) that they do not interfere with the solutions. To get some idea of how far the profiles have moved, note that the three maxima are each $30\Delta x$ apart. Thus, for example, the initial position of the Gaussian peak was half-way between the final positions of the sine-squared and semi-ellipse maxima.

Figure 5 shows the results of using first-order upwinding. Because of strong artificial diffusion (spatial second derivative) in the truncation error, the computed profiles have strongly interacted. Individually, the step simulation would look like a spreading error-function, whereas the other profiles soon degenerate into spreading (and amplitude-decaying) Gaussians, since all short-wavelength components in the original profiles are quickly damped out.

If one defines the grid Peclet number as

$$P_\Delta = u\Delta x/D \qquad (17)$$

where D is the physical diffusion coefficient, it is clear that the physical problem under consideration corresponds to infinite P_Δ. As is well known [26], first-order upwinding for infinite P_Δ is indistinguishable from any higher order method with an effective grid Peclet number given by

$$P_\Delta{}^* = 2/(1-c) \qquad (18)$$

In other words, for transient problems, first-order upwinding introduces artificial numerical diffusion of the form

$$D_{num} = u\Delta x(1-c)/2 \qquad (19)$$

Such artificially diffusive results should be recognized as being totally unacceptable. It is indeed rather surprising that such inaccurate methods are still the industry standard in many branches of computational engineering, especially numerical convective heat transfer [27,28].

Figure 6 shows results for the explicit second-order central Lax-Wendroff [4] scheme. In this case, there is a large phase lag due to the spatial third-derivative term in the truncation error. Only the smooth (sine-squared) profile bears any resemblance to the corresponding exact solution. Clearly, for highly convective flows, the explicit Lax-Wendroff method is very disappointing for all but the smoothest of profiles. The situation is not improved by using explicit second-order upwinding, shown in Figure 7. In this case, the third-derivative truncation-error terms are of opposite sign to those of the Lax-Wendroff method, resulting in phase-lead dispersion. For Courant numbers near 0.5, the individual second-order upwind results are almost a reflection of the Lax-Wendroff profiles.

7

Implicit second-order convection schemes are not necessarily better than explicit methods. The so-called "Crank-Nicolson-type" convection scheme [26] – defined by analogy with the well-known method for the diffusion equation [29] – is actually worse than explicit methods in the purely convective case, because there are strong phase-lag dispersion terms and no (even-derivative) dissipation terms in the truncation error. The highly oscillatory nature of this method is seen in Figure 8. The second-order implicit linear-finite-element method [26], shown in Figure 9, again has no dissipation but gives somewhat better results than other second-order methods because the leading third-derivative dispersion term is smaller.

Clearly, it would seem somewhat more felicitous to design a high-convection scheme in which the oscillatory third-derivative dispersion term in the truncation error were entirely eliminated. This was achieved over ten years ago in a simple explicit formulation known as the QUICKEST scheme [5]. In this case, leading truncation error is a small (fourth-derivative) dissipation term which strongly damps any dispersive tendencies of the non-zero fifth-derivative term without corrupting the modelled physics, *viz.*: the *absence* of physical (second-derivative) diffusion terms. Figure 10 shows a dramatic improvement over the dispersive second-order methods. Note particularly the good phase behaviour (which is relatively insensitive to Courant number). For reference, Figure 11 shows results for an explicit fourth-order central method [24]. Phase-lag dispersion in this case stems from the leading fifth-derivative truncation error (which is only lightly damped by higher order dissipation). Results are only slightly better than those of the best second-order method.

At the risk of belabouring the point, the above results seem to indicate fairly clearly that third-order upwinding represents a much more rational basis for CFD [6] than first- or second-order methods or higher order central schemes. As mentioned previously, there are still two serious short-comings, both evident in Figure 10: (i) unphysical undershoots or overshoots near regions of rapid change in gradient (high curvature); (ii) a limit to short-wavelength resolution. The first of these deficiencies can be overcome by applying the universal limiter; Figure 12 shows the resulting ULTIMATE QUICKEST computation. Step resolution is monotonic and comparable to that of MUSCL, Figure 13, a limited form of Fromm's method. (One should note that at $c = 0.5$, Fromm's method is equivalent to QUICKEST [24]). But it is clear that MUSCL tends to clip and flatten local extrema more strongly. This is directly linked to the more restrictive conditions imposed by the commonly used "TVD" limiter, given by (13).

The second deficiency of third-order upwinding can, of course, be corrected by using higher order (upwind) methods. The strategy proposed here is to use an appropriate higher order method *locally*, with third-order upwinding in relatively "smooth" (low-curvature) regions. For reference, Figure 14 shows results for (unlimited) ninth-order upwinding [24] used globally; ninth-order appears to be necessary to fully capture the peak of the narrow Gaussian. But, of course, this is an unlimited scheme, and undershoots and overshoots are excited near discontinuities. ULTIMATE ninth-order, Figure 15, eliminates the oscillations and gives very tight step-resolution, but again introduces slight clipping at extrema. If one could somehow arrange to automatically switch off the limiter near local extrema (while keeping it active near discontinuities), a very desirable convection scheme would result. This is the job of an adaptive discriminator which can distinguish between well-defined local physical extrema and short-wavelength spurious oscillations. Note that long-wavelength numerical oscillations, such as those occurring in second-order simulations – which might otherwise "confuse" the discriminator – present no problem (because they are excluded from the basic scheme).

8

CONSTRUCTION OF THE DISCRIMINATOR

The following algorithm attempts to distinguish between artificial numerical peaks, such as those potentially occurring near the step or the base of the semi-ellipse, and true physical extrema, such as those of the exact profiles in the test cases studied. Artificial peaks would be associated with short-wavelength numerical oscillations, with rapidly changing value, gradient, and curvature; as mentioned above, long-wavelength numerical oscillations are excluded from the third/higher order algorithm. If a local extremum is associated with short-wavelength oscillations, the discriminator chooses the limited algorithm; however, if the curvature is of the same sign in adjacent regions, the discriminator relaxes the limiter constraints at the extremum and the immediate upstream and downstream adjacent nodes.

In setting up the convective fluxes (for the right-face of each CV cell), consider an increasing-i "DO-loop" sweep. For the discriminator, choose a stencil of seven points: ϕ_{i-3}, ϕ_{i-2}, ϕ_{i-1}, ϕ_i, ϕ_{i+1}, ϕ_{i+2}, ϕ_{i+3}. Then compute the differences between each pair of consecutive points:

$$D1 = (\phi_{i-2} - \phi_{i-3}), \quad D2 = (\phi_{i-1} - \phi_{i-2}), \ldots, \quad D6 = (\phi_{i+3} - \phi_{i+2}) \qquad (20)$$

For convenience, assume there is a local maximum; a minimum requires reversal of some of the subsequent inequalities. Limiter constraints are active unless otherwise stated. The algorithm proceeds as follows:.

(i)   Check if D1 and D2 are both positive and D3 and D4 both negative; if not, go to step (iii); if they are, then:

(ii) Check if $|D2| < |D1|$ and $|D3| < |D4|$; if true, switch to an unlimited version at the current i-value and skip the remaining steps; otherwise:

(iii) Check if D2 and D3 are both positive and D4 and D5 both negative; if not, go to step (v); if they are, then:

(iv) Check if $|D3| < |D2|$ and $|D4| < |D5|$; if true, switch to an unlimited version at the current i-value and skip the remaining steps, otherwise:

(v)   Check if D3 and D4 are both positive and D5 and D6 both negative; if not, keep limiter constraints active; if they are, then:

(vi) Check if $|D4| < |D3|$ and $|D5| < |D6|$; if true, switch to an unlimited version at the current i-value; if not, proceed with the limiter constraints active.

Figure 16(a) shows a sketch of a case in which the discriminator would keep the universal limiter activated; in Figure 16(b), the limiter constraints would be removed at each of the points shown by a hollow circle. The discriminator routine is by-passed unless one of ϕ_{i+1}, ϕ_i, or ϕ_{i-1} is a local extremum. As noted above, limiter relaxation occurs (if at all) in groups of three points, with the discrete extremum in the middle.

ADAPTIVE STENCIL EXPANSION

The ultimate convection scheme proposed here uses the unlimited QUICKEST (third-order upwind) algorithm in smooth non-steep regions; i.e., wherever the average (right-face) absolute "curvature"

$$CURVAV = 0.5 \, |\phi_{i+2} - \phi_{i+1} - \phi_i + \phi_{i-1}| \qquad (21)$$

9

and "gradient"

$$GRAD = |\phi_{i+1} - \phi_i| \qquad (22)$$

are both less than pre-assigned thresholds, and provided [24]

$$0.2 \leq \tilde{\phi}_C \leq 0.8 \qquad (23)$$

If CURVAV exceeds THC1 or the larger THC2, the algorithm automatically switches locally (at the CV face in question) to ULTIMATE seventh- or ninth-order upwinding, respectively. If GRAD exceeds THG it locally switches directly to ULTIMATE ninth-order upwinding. This order-switching strategy is sketched in Figure 17. Also, if the limits expressed in (23) are locally exceeded, the limiter constraints are activated for the basic third-order scheme. Near local extrema, the discriminator automatically relaxes the limiter constraints, as described in the previous section. Clearly, the (dimensional) threshold constants need to be chosen carefully so as to capture the desired degree of accuracy without "overkill" in terms of cost; this requires some experimentation for optimization; a more universal (nondimensional) procedure is currently being explored.

Adaptive stencil expansion is a very cost-effective strategy because the wider-stencil computations are performed only where needed – at a relatively small number of grid points in narrow regions, by definition. This is even more effective in two and three dimensions. Figure 18(a) shows results for the complete algorithm; the small arrows show where the automatic discriminator has relaxed the limiter constraints (at this particular time-step). Figure 18(b) shows the corresponding distribution of GRAD, and 18(c) that of CURVAV. Finally, Figure 18(d) shows the local order of the algorithm to be used (at the next time-step) for the threshold constants chosen. It should be clear that the locations of the limiter-relaxation points and the order-switches move along with the profiles automatically, as time progresses.

CONCLUSION

A cost-effective strategy for high-convection modelling has been introduced. The algorithm is based on the (third-order upwind) QUICKEST scheme in smooth regions, as this is the lowest order method in which the leading truncation error is dissipative but not diffusive. QUICKEST's phase error is relatively low, but overshoots or undershoots can be excited by the unlimited scheme near discontinuities, and short-wavelength resolution would, of course, be limited to third order. A more sophisticated scheme is therefore devised in which monotonicity is guaranteed by a universal limiter which can be applied to any order of accuracy. Appropriate degrees of higher order resolution are automatically introduced locally, using adaptive stencil expansion controlled by monitoring local (absolute) gradient and curvature of the convected variable. Potential clipping of narrow extrema is avoided by automatic relaxation of the limiter constraints in local regions based on pattern-recognition decisions of an adaptive discriminator. By judicious choice of threshold constants, the overall method can produce extremely accurate results on a coarse mesh at relatively little additional cost above that of the base third-order scheme. The same principles can be applied to multidimensional flows and non-linear systems. Work is proceeding on these applications.

REFERENCES

1. Mitchell, A.R.: Recent Developments in the Finite Element Method. *Computational Techniques and Applications: CTAC-83*, J. Noye and C.A.J. Fletcher, eds., Elsevier North-Holland, 1984, pp. 2-14.

2. Courant, R.; Isaacson, E.; and Rees, M.: On the Solution of Nonlinear Hyperbolic Differential Equations by Finite Differences. *Commun. Pure Appl. Math.*, Vol. 5, 1952, pp. 243-255.

3. Fromm, J.E.: A Method for Reducing Dispersion in Convective Difference Schemes. *J. Comput. Phys.*, Vol. 3, 1968, pp. 176-189.

4. Lax, P.D.; and Wendroff, B.: Systems of Conservation Laws. *Commun. Pure Appl. Math.*, Vol. 13, 1960, pp. 217-237.

5. Leonard, B.P.: A Stable and Accurate Convective Modelling Procedure Based on Quadratic Upstream Interpolation. *Comput. Methods Appl. Math. Eng.*, Vol. 19, No. 1, June 1979, pp. 59-98.

6. Leonard, B.P.: Third-Order Upwinding as a Rational Basis for Computational Fluid Dynamics. *Computational Techniques and Application: CTAC-83*, J. Noye and C.A.J. Fletcher, eds., Elsevier North-Holland, 1984, pp. 106-120.

7. Anderson, D.A.; Tannehill, J.C.; and Pletcher, R.H.: *Computational Fluid Mechanics and Heat Transfer*, Hemisphere Publishing Corp., Washington, D.C., 1984.

8. Gosman, A.D.; and Pun, W.M.: Lecture Notes for a Course Entitled: Calculation of Recirculating Flows. Heat Transfer Section Report HTS/74/2, Imperial College Mechanical Engineering Dept., 1974.

9. Spalding, D.B.: A Novel Finite Difference Formulation for Differential Expressions Involving Both First and Second Derivatives. *Int. J. Numer. Methods Eng.*, Vol. 4, No. 4, July-Aug. 1972, pp. 551-560.

10. Raithby, G.D.; and Schneider, G.E.: Elliptic Systems: Finite-Difference Method II. *Handbook of Numerical Heat Transfer*, W.J. Minkowycz, et al., eds., Wiley, 1988, pp. 241-291.

11. Patankar, S.V.: *Numerical Heat Transfer and Fluid Flow*, Hemisphere Publishing Corp., Washington, D.C., 1980.

12. Syed, S.A.; Gosman, A.D.; and Peric, M.: Assessment of Discretization Schemes to Reduce Numerical Diffusion in the Calculation of Complex Flows. AIAA Paper 85-0441, Jan. 1985.

13. de Vahl Davis, G.; and Mallinson, G.D.: An Evaluatin of Upwind and Central Difference Approximations by a Study of Recirculating Flow. *Comput. Fluids*, Vol. 4, No. 1, Mar. 1976, pp. 29-43.

14. Raithby, G.D.: A Critical Evaluation of Upstream Differencing Applied to Problems Involving Fluid Flow. *Comput. Methods Appl. Mech. Eng.*, Vol. 9, No. 1, Sept. 1976, pp. 75-103.

15. Leonard, B.P.: A Consistency Check for Estimating Truncation Error Due to Upstream Differencing. *Appl. Math. Modelling*, Vol. 2, No. 4, Dec., 1978, pp. 239-244.

16. Huang, P.G.; Launder, B.E.; and Leschziner, M.A.: Discretization of Non-Linear Convection Processes: A Broad-Range Comparison of Four Schemes. *Comput. Methods Appl. Mech. Eng.*, Vol. 48, No. 1, Feb. 1985, pp. 1-24.

17. Leschziner, M.A.: Practical Evaluation of Three Finite Difference Schemes for the Computation of Steady-State Recirculating Flows. *Comput. Methods Appl. Mech. Eng.*, Vol. 23, No. 3, Sept. 1980, pp. 293-312.

18. Yee, H.C.: Upwind and Symmetric Shock-Capturing Schemes. NASA TM-89464, 1987.

19. Boris, J.P.; and Book, D.L.: Flux-Corrected Transport III. Minimal-Error FCT Algorithms. *J. Comput. Phys.*, Vol. 20, No. 4, Apr. 1976, pp. 397-431.

20. van Leer, B.: Towards the Ultimate Conservative Difference Scheme. V. A Second-Order Sequel to Godunov's Method. *J. Comput. Phys.*, Vol. 32, 1979, pp. 101-136.

21. Leonard, B.P.: Adjusted Quadratic Upstream Algorithms for Transient Incompressible Convection. *AIAA 4th Computational Fluid Dynamics Conference*, AIAA, 1979, pp. 226-233.

22. Leonard, B.P.: A Survey of Finite Differences with Upwinding for Numerical Modelling of the Incompressible Convective Diffusion Equation. *Computational Techniques in Transient and Turbulent Flow*, C. Taylor and K. Morgan, eds., Pineridge Press, 1981, pp. 1-36.

23. Roe, P.L.: Some Contributions to the Modelling of Discontinuous Flows. *Large Scale Computations in Fluid Mechanics, Part 2 (Lectures in Applied Mathematics, Vol. 22)*, B.E. Engquist, S. Osher, and R.C.J. Somerville, eds., American Mathematical Society, Providence, RI, 1985, pp. 163-193.

24. Leonard, B.P.: Universal Limiter for Transient Interpolation Modeling of the Advective Transport Equations: The ULTIMATE Conservative Difference Scheme. NASA TM 100916 (ICOMP-88-11), 1988.

25. Sweby, P.K.: High Resolution Schemes Using Flux Limiters for Hyperbolic Conservation Laws. *SIAM J. Numer. Anal.*, Vol. 21, No. 5, Oct. 1984, pp. 495-1011.

26. Fletcher, C.A.J: *Computational Techniques for Fluid Dynamics*, Springer-Verlag, 1988.

27. Minkowycz, W.J.; *et al.*: eds., *Handbook of Numerical Heat Transfer*, Wiley, 1988.

28. Lewis, R.W.; and Morgan, K.: eds., *Numerical Methods in Thermal Problems VI*, Pineridge Press, 1989.

29. Crank, J.; and Nicolson, P.: A Practical Method for Numerical Evaluation of Solutions of Partial Differential Equations of the Heat-Conduction Type. *Proc. Cambridge Philos. Soc.*, Vol. 43, Pt. 1, Jan. 1947, pp. 50-67.
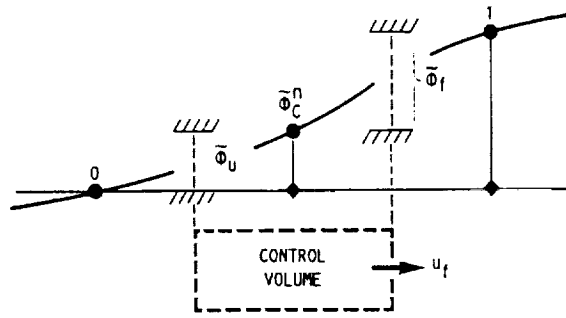
FIGURE 1   Locally monotonic behaviour across a control-volume cell in terms
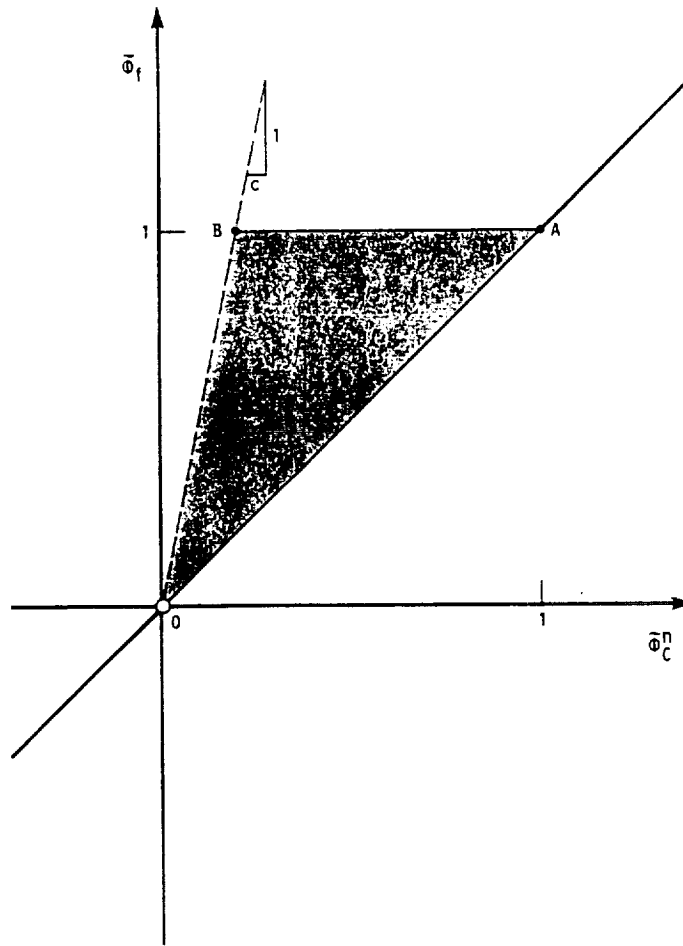of normalized variables.

FIGURE 2   Universal limiter constraints in the normalized-variable diagram.
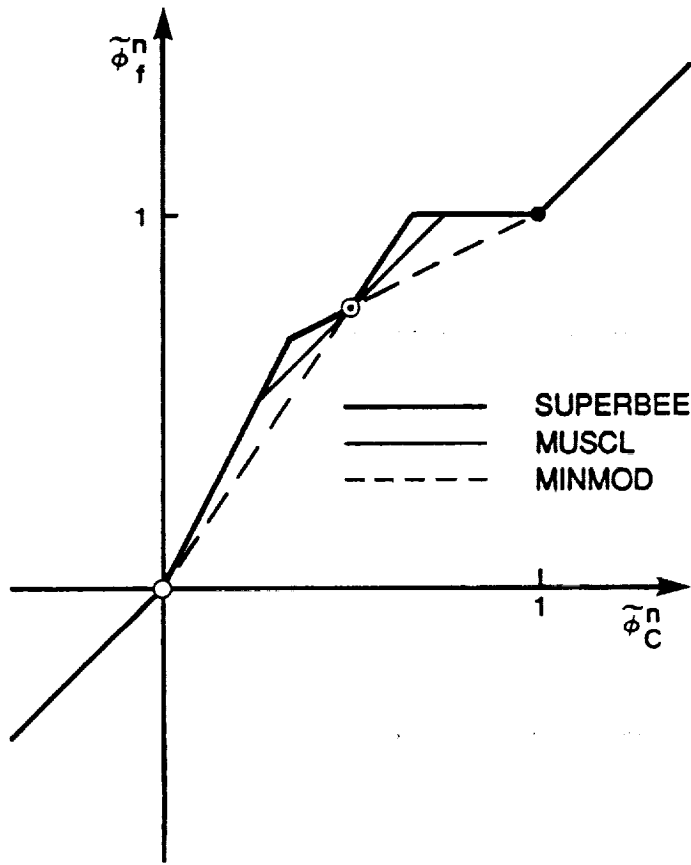
13

FIGURE 3   Normalized variable diagrams for Superbee (heavy lines), Minmod
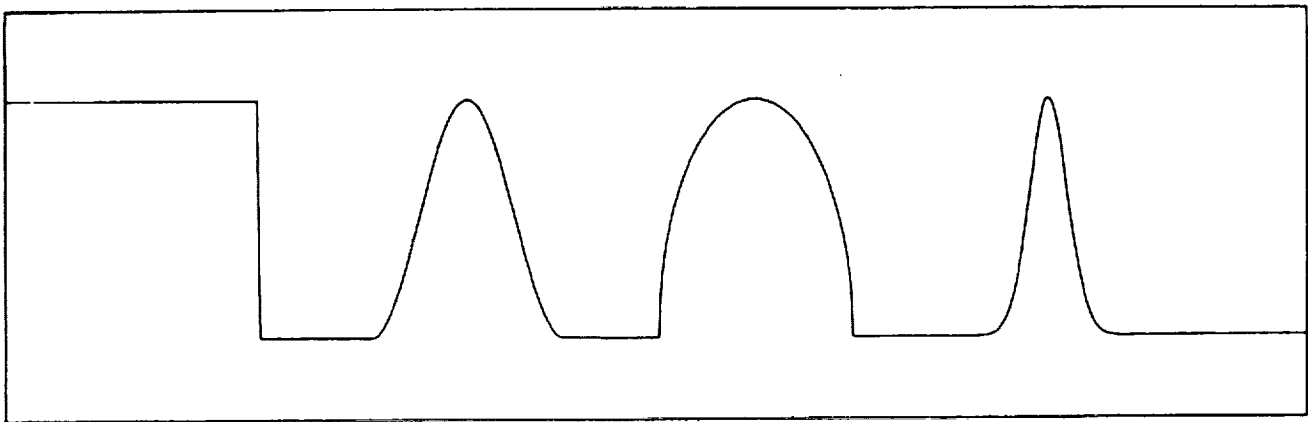
(dashed), and MUSCL.

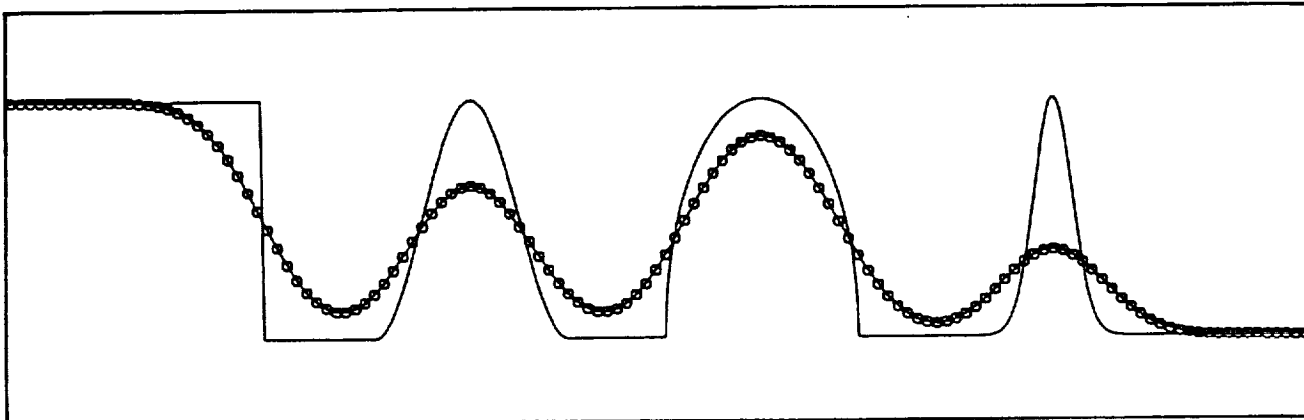FIGURE 4   Exact solution for the four scalar test profiles considered.

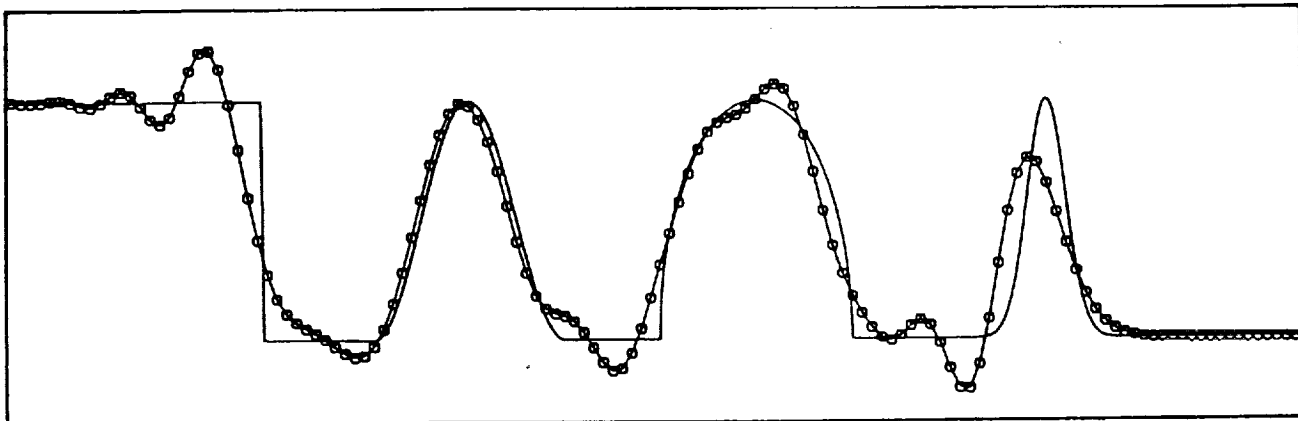FIGURE 5   First-order upwind results compared with exact solution.
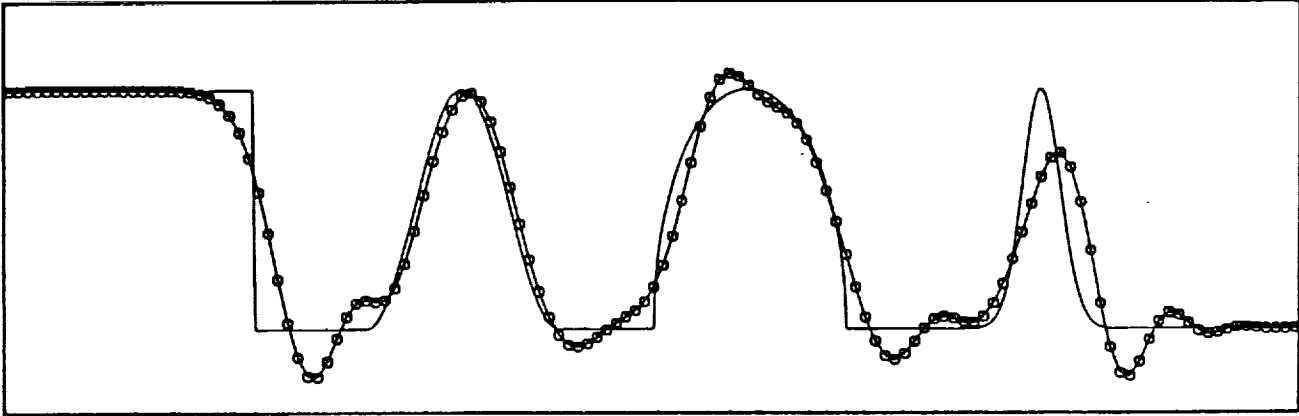

FIGURE 6   Lax-Wendroff results compared with exact solution.

15

FIGURE 7   Second-order upwind results compared with exact solution.
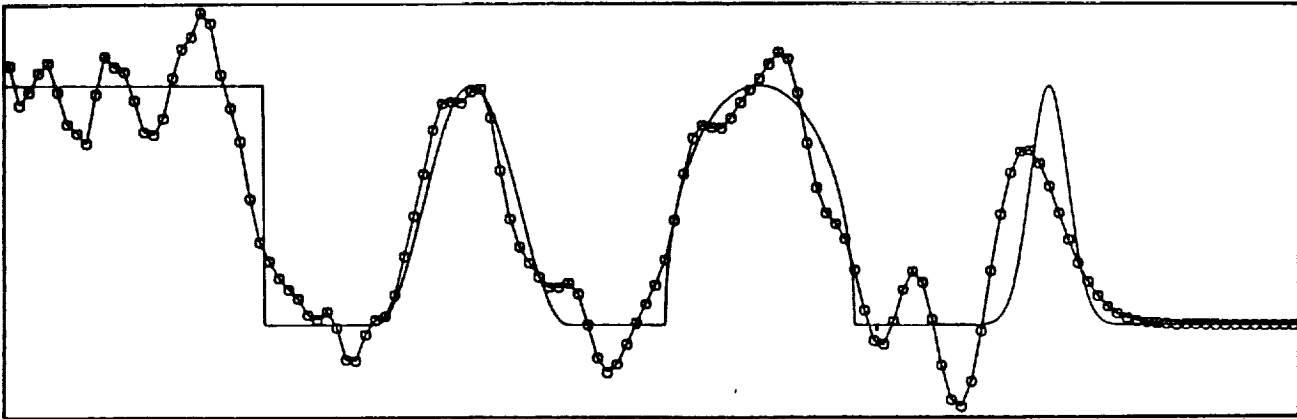
FIGURE 8   Crank-Nicolson results compared with exact solution.

16
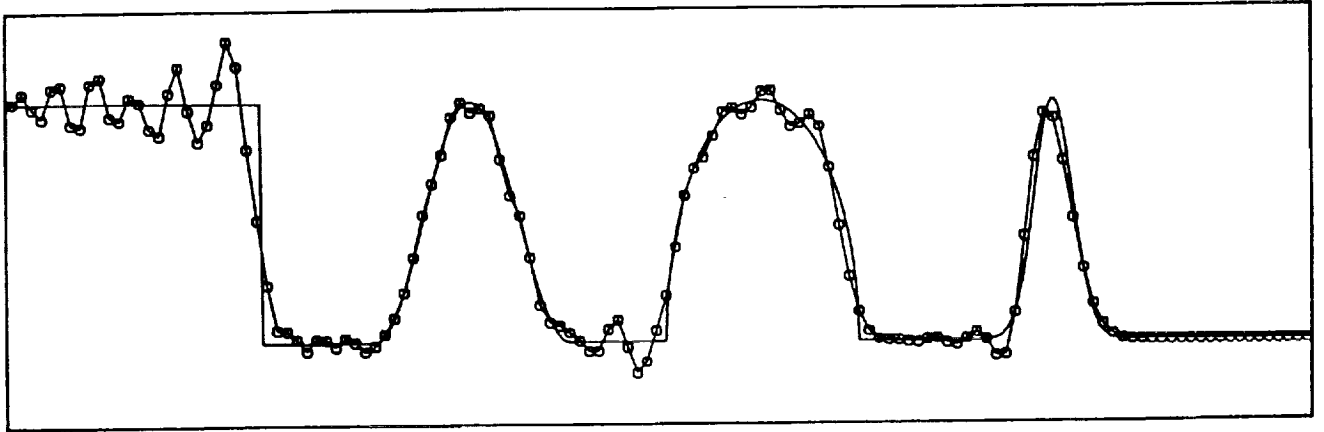
FIGURE 9   Linear-finite-element results compared with exact solution.
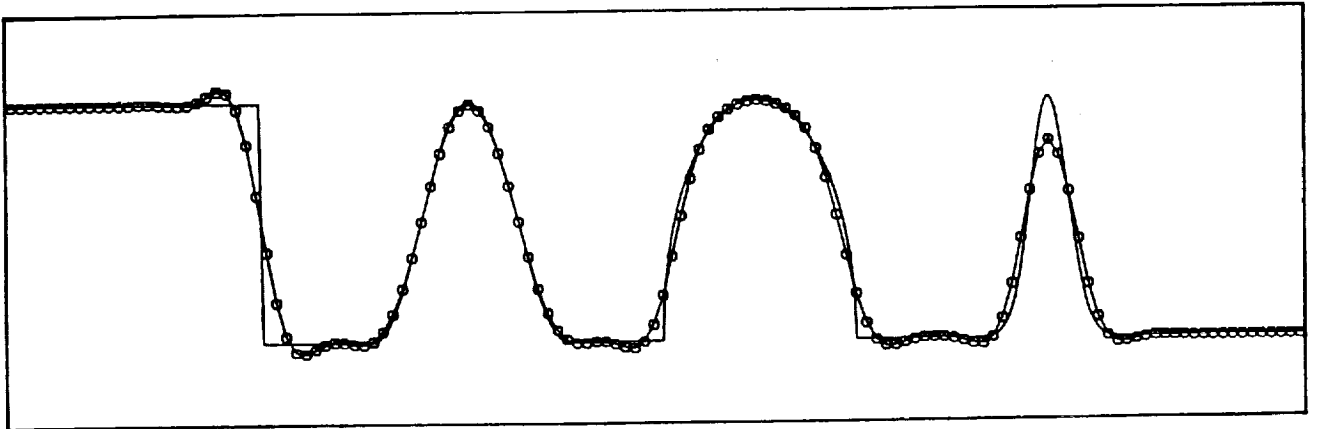
FIGURE 10   Third-order upwind (QUICKEST) results compared with exact
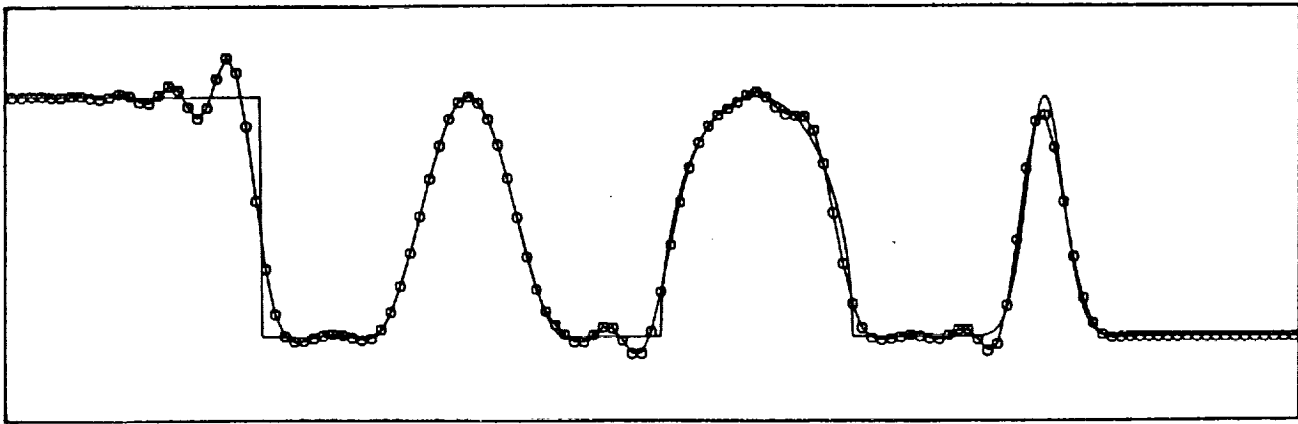
solution.

FIGURE 11   Fourth-order central results compared with exact solution.
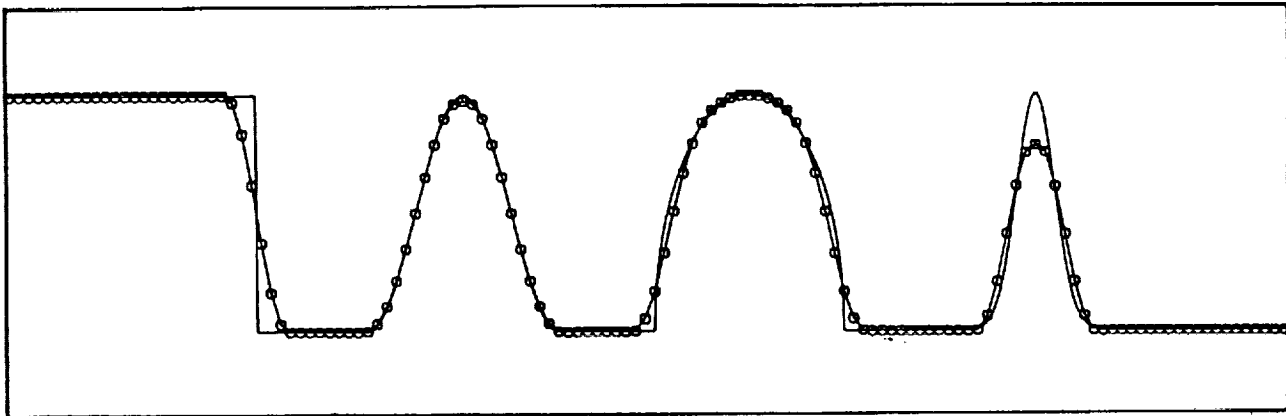
FIGURE 12   ULTIMATE QUICKEST results compared with exact solution.

18
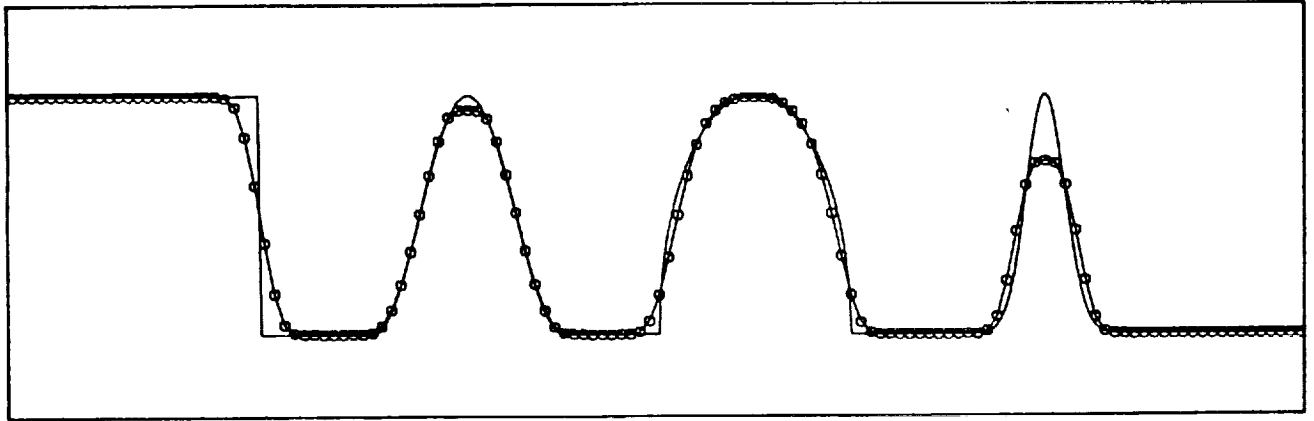
FIGURE 13   Results using MUSCL compared with exact solution.
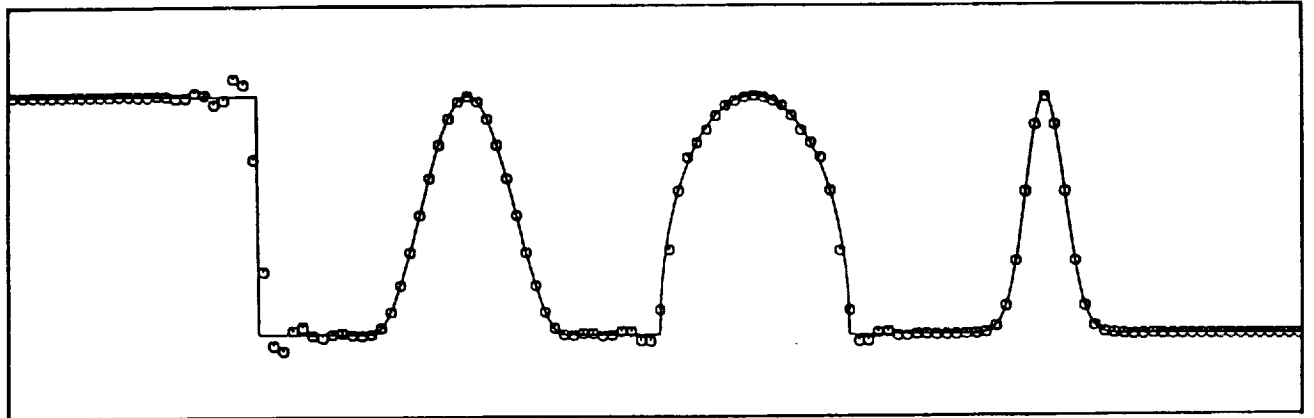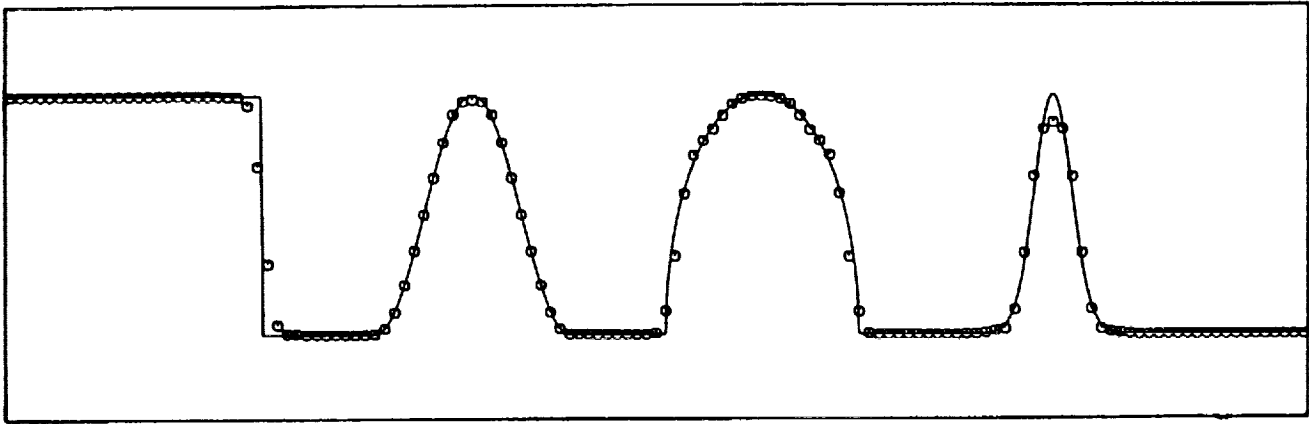

FIGURE 14   Unlimited ninth-order upwinding.

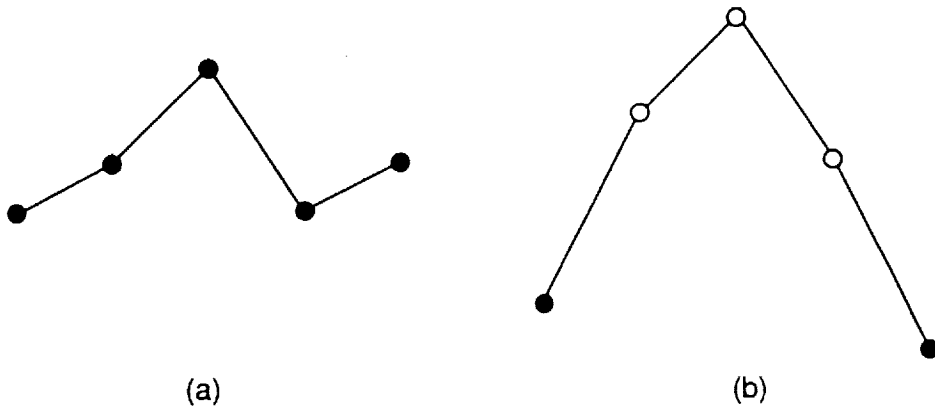FIGURE 15   ULTIMATE ninth-order upwinding.

(a)   (b)

FIGURE 16   Action of the discriminator. (a) Limiter switched on.

(b) Limiter switched off at three central points.
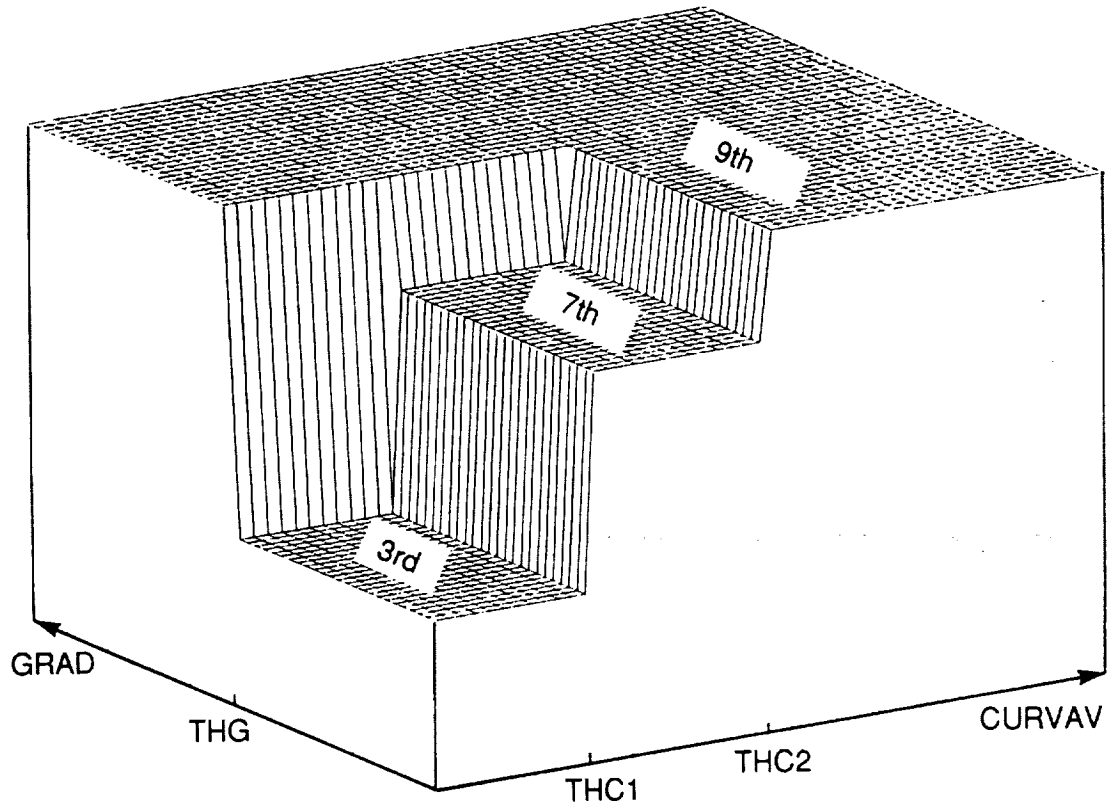
FIGURE 17   Schematic of order-switching strategy in terms of CURVAV and GRAD.
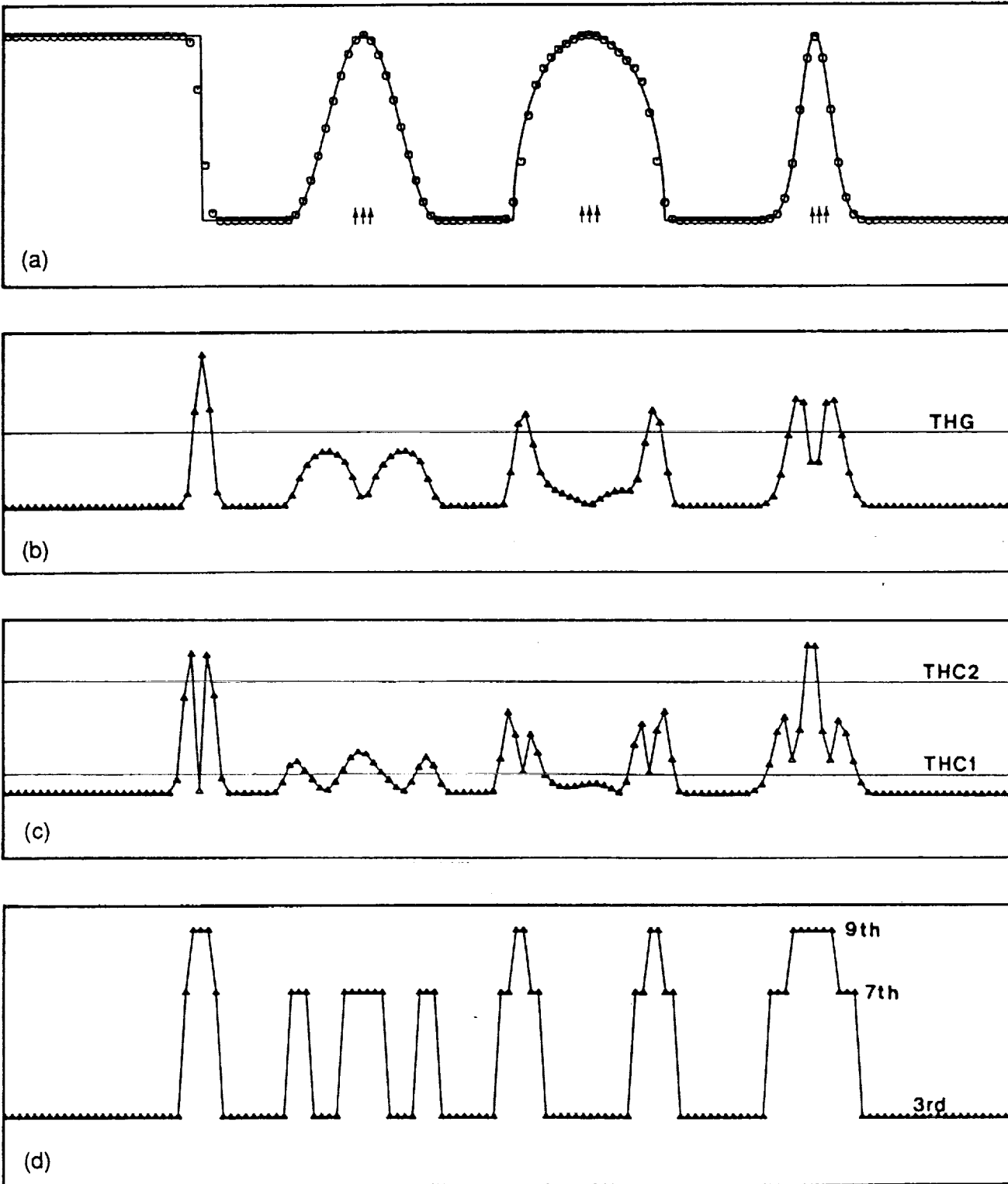
FIGURE 18   Third/higher-order adaptive scheme with discriminator.

(a) Computed results. (b) Distribution of GRAD relative to THG.

(c) Distribution of CURVAV relative to THC1 and THC2.

(d) Order of the algorithm to be used locally in next time-step.

Report Documentation Page

1. Report No. NASA TM-102538 ICOMP-90-09	2. Government Accession No.	3. Recipient's Catalog No.
4. Title and Subtitle A Cost-Effective Strategy for Nonoscillatory Convection Without Clipping		5. Report Date March 1990
		6. Performing Organization Code
7. Author(s) B.P. Leonard and H.S. Niknafs		8. Performing Organization Report No. E-5336
		10. Work Unit No. 505-62-21
9. Performing Organization Name and Address National Aeronautics and Space Administration Lewis Research Center Cleveland, Ohio 44135-3191		11. Contract or Grant No.
		13. Type of Report and Period Covered Technical Memorandum
12. Sponsoring Agency Name and Address National Aeronautics and Space Administration Washington, D.C. 20546-0001		14. Sponsoring Agency Code

16. Abstract

Clipping of narrow extrema and distortion of smooth profiles is a well-known problem associated with so-called "high-resolution" nonoscillatory convection schemes. In this report, a strategy is presented for accurately simulating highly convective flows containing discontinuities such as density fronts or shock waves, without distorting smooth profiles or clipping narrow local extrema. The convection algorithm is based on non-artificially-diffusive third-order upwinding in smooth regions, with automatic adaptive stencil expansion to (in principle, arbitrarily) higher order upwinding locally, in regions of rapidly changing gradients. This is highly cost-effective because the wider stencil is used only where needed-in isolated narrow regions. A recently developed universal limiter assures sharp monotonic resolution of discontinuities without introducing artificial diffusion or numerical compression. An adaptive discriminator is constructed to distinguish between spurious overshoots and physical peaks; this automatically relaxes the limiter near local turning points, thereby avoiding loss of resolution in narrow extrema. Examples are given for one-dimensional pure convection of scalar profiles at constant velocity.

17. Key Words (Suggested by Author(s)) Upwind schemes High-order convection Nonoscillatory convection Clipping eliminated	18. Distribution Statement Unclassified – Unlimited Subject Category 34	
19. Security Classif. (of this report) Unclassified	20. Security Classif. (of this page) Unclassified	21. No. of pages 24	22. Price* A03